ISSN: 2633-4828 Vol. 6 No.1, January, 2024

International Journal of Applied Engineering & Technology

THE INVESTIGATION OF ELECTROCHEMICAL CORROSION OF STEEL REBARS IN A CONCRETE ENVIRONMENT

Mohammed Saleh Al Ansari
Department of Chemical Engineering, College of Engineering, University of Bahrain,
PO Box 32038, Sukhair Campus, Kingdom of Bahrain
malansari@uob.edu.bh

ABSTRACT

There was simultaneous recording of the potential and current Electro Chemical Noise (ECN) that was produced by steel rebar in cement solution. Calculations were performed in both the time and frequency domains to determine the average potential, the noise power of the current, and the anticipated charge during the transient condition. ECN of rebar in pure water and a solution containing chloride were used to compare the findings with one other. A proposal has been made to examine the results with an enhanced signal-to-noise ratio in the article that we will be writing in the future.

Keywords: Electro Chemical Noise (ECN), steel rebar, cement solution

1. INTRODUCTION

There are instances of damage that can be seen in the majority of applications of reinforced or prestressed concrete that are caused by corrosion of the rebar. It is the spalling of the concrete that is the manifestation of the corrosion that occurs in reinforcement that is embedded in concrete. It is because of the expanding character of the corrosion products that this phenomenon occurs. These products are capable of producing enormous stresses without a significant loss of surface area. There is a secondary reaction that takes place between $2Fe_2(OH)_2$ and oxygen from the air, which results in the formation of expanding red rust products. These have the ability to separate from the surface of the steel. The smaller cross section of corroded steel bars can also lead to structural failure, which is another potential consequence of the corrosion process. When taking into consideration the enormous amount of money that is lost due to the corrosion of rebar, it is essential to take into account the numerous internal and external aspects that are responsible for the corrosion of steel bars in concrete. It is believed that electrochemical corrosion is the cause of virtually all of the corrosion damage that occurs to steel in concrete. The occurrence of electrochemical corrosion in concrete is a consequence of the presence of differences in metals, non-uniformities of the steel, or non-uniformities in the chemical or physical environment that is provided by the concrete that is surrounding the concrete. These types of non-uniformities have the ability to generate considerable electrical potential variations, which can then lead to corrosion Jiyue Hu, 2021. A flow of current in the steel from an anodic area to a cathodic area, in the presence of oxygen and moisture, resulting in the generation of hydroxyl ions at the cathode. This occurs because the aluminium is oxidised. On their way to the anode, they undergo a reaction with ferrous iron, which results in the formation of hydrous iron oxides.

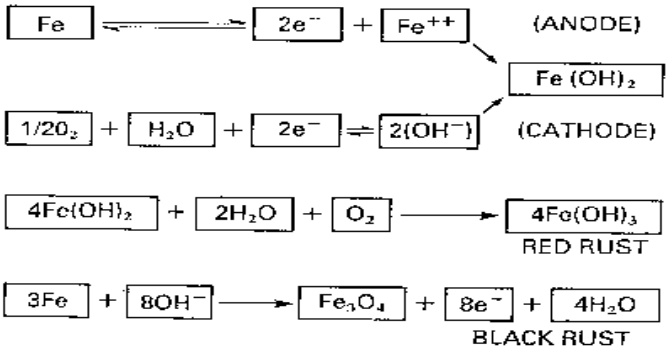

Fig. 1 Electrochemical reactions producing rust.

It is evident from the aforementioned equations that the presence of oxygen and water is essential for corrosion to take place. However, the majority of constructional concretes facilitate generous permeation of both water and oxygen. According to the conventional perspective, corrosion is typically hindered by the formation of a protective iron oxide film (gamma Fe_2O_3) on the surface of steel. This film develops quickly when there is moisture, oxygen, and water-soluble alkaline compounds present during the cement hydration process. The primary soluble compound formed is calcium hydroxide, $Ca(OH)_2$, and the initial alkalinity of the concrete exceeds 12.5. The protective layer maintains its integrity at elevated pH levels, about around 13 according to Akib Jabed et al,2023. The steel is protected by a high pH value, which continues to be effective while the concrete sets and hardens. This protection remains intact as long as there are no substantial changes in the concrete environment surrounding the steel. After the concrete has fully dried and reached a stable moisture level, the steel's protection relies only on the concrete's ability to sustain the necessary alkaline conditions. Nevertheless, the integrity of the protective film composed of γ-Fe_2O_3 on the steel surface is typically compromised when the pH value decreases or when hostile ions infiltrate due to capillary action, concrete cracking and spalling, substandard construction procedures, or a combination of these causes. When the protective cover is disrupted, it causes corrosive damage to the reinforcement. After the attack begins, the steel surface experiences the accumulation of corrosion products. The loss of alkalinity occurs when the cement matrix reacts with acidic components in the atmosphere and when hydroxyl ions are partially washed out from the concrete. When the pH of the matrix decreases to a value between 9.5 and 10 Steel can undergo corrosion when exposed to sufficient amounts of moisture (to facilitate the electrolytic pathway) and oxygen (to trigger the cathodic reaction). Aggressive ions have the ability to eliminate passivity. Chloride is the most corrosive ion when it comes to steel corrosion. If there is enough chloride in concrete, it may easily break down the protective layer on the steel, causing fast and severe corrosion. Due of its porosity, concrete permits the entry of atmospheric gases. These substances will contain carbon dioxide, which will easily react with the alkaline substances present, hence decreasing the pH. The degree of entry, along with other parameters, will be regulated by the permeability of both the concrete matrix and the aggregate. Carbonation and the presence of chloride in the concrete are two factors that can lead to the loss of protection to the reinforcement. Chlorides can be introduced into concrete through several means. In the Middle East, chlorides are typically present in concrete as impurities in the aggregate, mix water, or due to exposure to environments with high chloride content. The most prevalent route among these is the one that goes through the aggregate. In addition to chlorides, Middle Eastern aggregates may also be polluted with sulphates. This poses an additional challenge in preventing potential sulphate attack on concrete.

1.1 General Corrosion

General corrosion is the result of general loss of passivity, due either to carbonation or the presence of excessive amounts of chloride. The potential gradients are not great. In general, the major cause of failure and deterioration in concrete construction is the corrosion of steel rebar. Over two kilogram of concrete are used per annum for every person on this earth. It has been shown that cement consumption may be diminished by constructing long-lasting buildings. Steel corrodes in damp environments because airborne contaminants seep through the concrete cover. Destruction to concrete from corrosion may increase its volume by a factor of six to eight compared to that of steel structure's failure Akib Jabed, 2023.

1.2 Localised Corrosion

Pitting corrosion is a type of localised corrosion caused by the breakdown of the protective oxide film in a specific area. Typically, chloride is present as a necessary component to initiate this breakdown. The passive film is chemically inert and has the ability to self-repair if it is accidentally damaged. Occasionally, certain regions of the passive coating can undergo permanent electrochemical or mechanical breakdown, enabling anions to attack the uncovered metal and causing localised corrosion. Pitting is a microscopic occurrence, meaning that it occurs at a very small scale. It involves significant rates of localised penetration, although the overall corrosion rate is quite low. Crevice corrosion is a type of localised damage that happens in protected places on metal surfaces when they

are exposed to specific conditions. This attack is typically linked to limited quantities of motionless liquid resulting from the presence of gasket surfaces, lap joints, holes, and crevices beneath bolts and rivet heads.

1.2.1 The State of Pitting Corrosion

In regions where the concentration is high or the passive film is weak, the chloride ions are responsible for the localized breakdown of the passive film. According to Mills, D.J. and Short, N.R. 2002, Jiyue Hu, 2021 the process of corrosion begins with the formation of a corrosion cell, which is accompanied by an adjacent area of passive steel that functions as a cathode. Within this cell, oxygen is decreased, and the anodic dissolution of iron occurs only at a small, central anode.

1.2.2 Growth of Pits

The following Figure for pitting of iron in a slightly alkaline chloride solution serves as a simplified model.

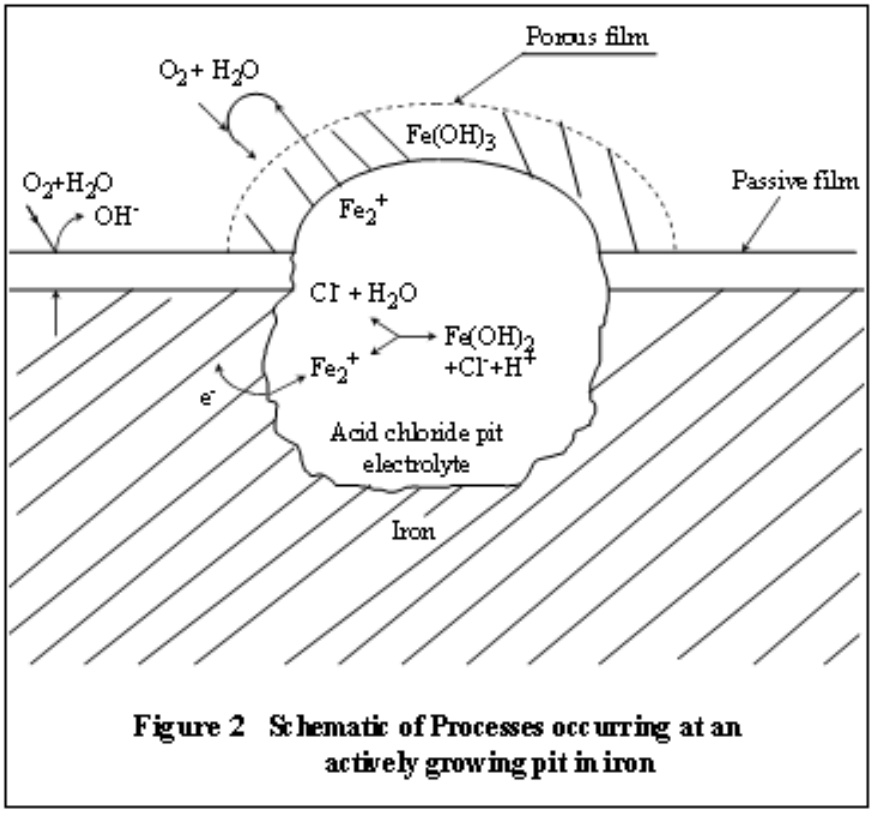

Figure 2 Schematic of Processes occurring at an actively growing pit in iron

Copious anodic production of positively charged Fe^{2+} attracts negative anions, eg., Cl^-, to the initiation site. Hydrolysis by

$$Fe^{2+} + 2H_2O + 2Cl^- = Fe(OH)_2 + 2HCl$$

causes a decrease in pH levels in the immediate vicinity of the starting site. The end result is a process of pit growth that is either self-propagating or autocatalytic for growth. A further acceleration of anodic dissolution is brought about by the acid chloride solution, which in turn brings about an even greater concentration of chloride in the pit. When Fe^{2+} diffuses out of the acid pit interior and into the exterior, it is oxidized to Fe3+ and precipitates in the neutral bulk solution. This resulted in the accumulation of an insoluble cap of Fe(OH)3 corrosion products at the pit mouth. A high acid chloride concentration is maintained in the pit as a result of the cap's ability to prevent the easy escape of Fe^{2+} while still being sufficiently porous to allow Cl^- to migrate into the pit. The coupling to the external passive cathode surfaces is what causes the anodic polarization of the pit interior

to take place. Cathodic reduction, which involves the consumption of electrons that have been freed by the anodic pit reaction, is performed on a dissolved oxidizer like oxygen. At the very least, until far larger chloride concentrations are generated in other areas, the formation of new pits in the neighborhood is prevented by a number of variables, one of which is the significant decrease in the corrosion potential that is brought about by the polarization of the cathode. On the other side, the possible change can also initiate the creation of a situation in which the attack is not allowed to proceed. As a result of the low pH liquid at the anode neutralizing the concrete at the rim of the anode, the current density at the anode will decrease. This is due to the fact that the driving force will be reduced, and the larger area of the anode will also grow. As a consequence of this, the concentration gradients that are formed electrochemically will be flattened by the diffusion of ions in the opposite direction, which may lead to the repassivation effect of the pit. Significant amounts of corrosion can take place without the concrete spalling as a result of the fact that the corrosion products that are generated are typically soluble in the conditions of low pH that are close to the anode. In order to maintain pitting, it is essential to have an understanding of the significance of the cathodic reaction. The growth of the pit cannot proceed without a cathodic reduction reaction, which is necessary in order to consume the electrons that are released as a result of the pit anode reaction, which causes the pit to polarize anodically. The reason for this is that oxygen has a limited solubility, and a vast surrounding area is required to give sufficient reduction capability to maintain the central pit anode. As a result, pits are widely spaced in aerated salt solutions. The cathodic protection measures are designed to prevent any pit from forming within the cathodic area of a larger pit. Using a potential-pH diagram, one may depict the reactions that occur when iron is present in aqueous solutions. Immunity, corrosion, and passivity are the three zones that can be separated out on a simplified potential-pH diagram.

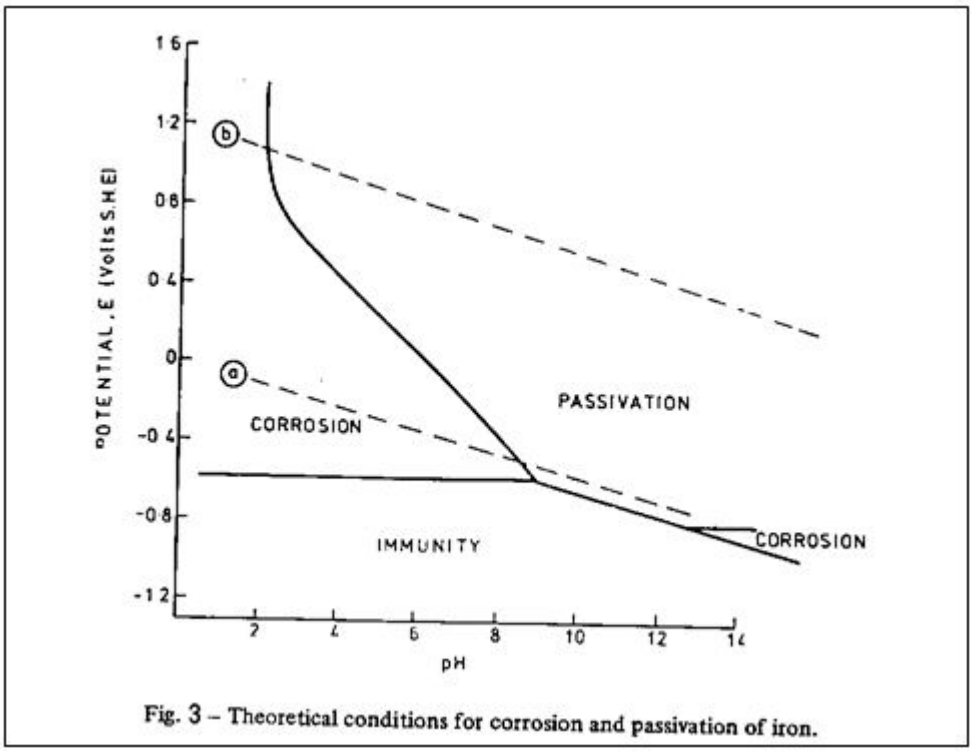

Fig. 3 – Theoretical conditions for corrosion and passivation of iron.

Chloride that has penetrated the surface of the steel does not necessarily result in the destruction of passivity. Pourbax presents a modified potential-pH diagram that demonstrates that even with extremely high chloride concentrations, a zone of perfect passivity is still present. Furthermore, it has been demonstrated that the corrosion of steel in concrete that is exposed to a high chloride environment can be prevented by polarizing to a potential within this zone.

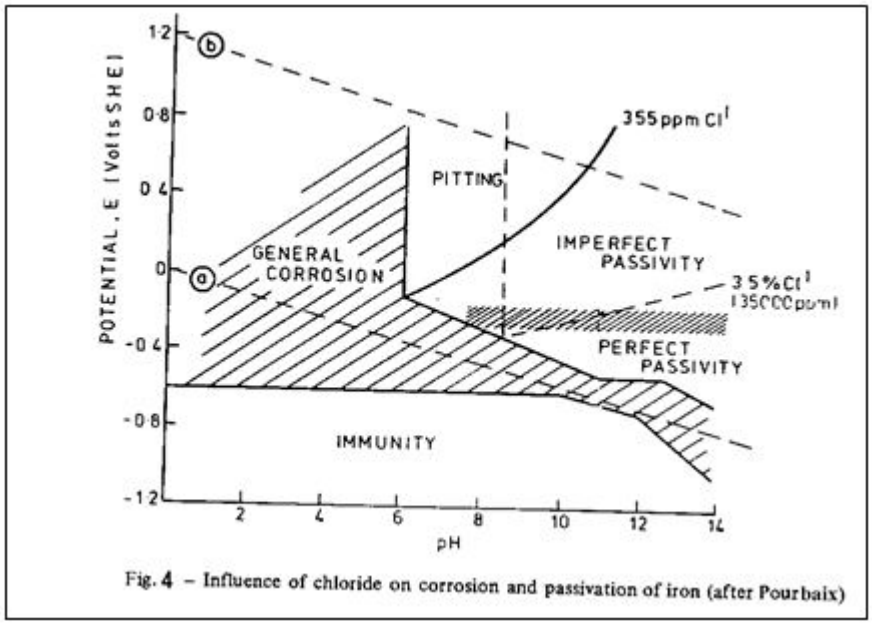

Fig. 4 – Influence of chloride on corrosion and passivation of iron (after Pourbaix)

The two principal cathodic reactions available for the corrosion of steel in concrete are indicated on the potential-pH diagrams:

Line (a) $2H^+ + 2e- \rightarrow H_2$

Line (b) $½ O_2 + H_2O + 2e^- \rightarrow 2OH^-$

However, oxygen reduction is recognised as the cathodic reaction in most cases of significant corrosion of steel reinforcement.

2. Corrosion Monitoring of Steel in Concrete

The investigation of corrosion in reinforced concrete can be accomplished through the use of a variety of scientific methods. The goals of the researcher should be taken into consideration when choosing the method to conduct the research. In the case of a material scientist who is interested in laboratory-based fundamental investigations, for instance, the requirements of the engineer who is concerned with a practical on-site assessment are slightly different from its goals. For the purpose of evaluating the extent of corrosion damage to existing structures, the examination would initially be used to quantify the extent of corrosion damage. This would be followed by a requirement to predict future performance. One of the most significant challenges is that there is no single method that provides sufficient information; consequently, there is a degree of discretion that is required when evaluating the vulnerability to corrosion. Traditional electrochemical approaches have been shown to be shockingly inappropriate for assisting in on-site monitoring, despite the fact that corrosion is a process that results from electrochemical reactions. In order to give the engineering data necessary for evaluating the current condition and predicting the performance over the long term, destructive tests have been relied upon for the inspection of structures. Measurements on the actual structural rebar are the first of the available techniques, and the second of these involves measurements on smaller, strategically positioned embedded rebar probes. The available techniques can be broadly split into two types.

2.1 Potential Mapping

Corrosion potential measurements, which involve placing a reference electrode (preferably calomel) on the surface of the concrete and connecting it to the reinforcement cage using a high input impedance voltmeter, are able to offer information regarding the level of passivity of the reinforcing steel. The measurement process for this approach is detailed in the American National Standard ANSI/ASTM C-876. The premise behind this technique is

that the corrosion potential of the rebar will shift in the opposite direction if the surface shifts from the passive state to the active state. This technique is by far the simplest of all the techniques. The simplicity of this technology, as well as the ability of automating measurements, confers an advantage that allows for the coverage of huge concrete surface areas in a very short amount of time. The fact that the data are solely qualitative and do not establish an actual rebar corrosion rate is one of the drawbacks of the study. In addition, measurements of rebar potential that are extremely negative might be deceiving and may be the result of oxygen diffusion which is exceedingly restricted. In buried concrete, for instance, where the corrosion rates are low, very negative potential readings are achievable due to the absence of oxygen, which stifles the cathodic corrosion rate. It is feasible for these values to be quite negative.

2.2 Potentiodynamic Sweep or Potential Step Measurements.

These well-known measurements of the direct current type can be carried out with the help of the traditional three electrode technique. A tiny part of the rebar is often employed as the working electrode, while graphite or stainless steel may be utilized as the counter electrode. It is essential that embedded reference electrodes have the ability to withstand the extremely alkaline pore solution. It is also possible to make use of external reference electrodes. Direct adoption for research in concrete, on the other hand, is susceptible to criticism unless it is taken into account both the high resistivity of the environment, which can be compensated for by IR drop compensation, and the very slow kinetics of the electrochemical corrosion reactions that occur on reinforcement steel. As a result, the typical potentiodynamic method would appear to have only a limited use. For instance, in first investigations, it is highly doubtful that it will give kinetic information or data that can be measured.

2.3 AC Impedance

The corrosion that occurs at the interface between concrete and steel is a complicated process. Therefore, it would appear that the impedance approach is the most suitable laboratory methodology. This method offers information on the kinetic control mechanisms, which can be either activation or diffusion, as well as on the electrochemical capacitive elements and the film dielectric components. The approach is able to measure the resistance of the pore solution or the concrete, in addition to the electrochemical parameters, which include the double layer capacitance, the charge transfer resistance, and the Warburg diffusion. The corrosion processes are defined by these parameters, and because each component reacts to the applied voltage perturbation within the given frequency ranges, it is possible to quantify each component. The technique known as electrochemical impedance is primarily a laboratory-based method that can be utilized for research on relatively small electrodes or sections of reinforcement bar.

2.4 Electrochemical Noise

Several localized corrosion events, including as pitting, abrasion, and gas development, occur randomly. Therefore, standard deterministic approaches such as I-E charting are not applicable. The electrochemical noise generates potential and current variations that follow a random or stochastic pattern, making it impossible to accurately forecast their exact values at a future moment in time. The data obtained from this phenomena exhibit a random nature and are therefore represented using probability assertions and statistical averages rather than explicit formulae. The level of noise generated by the deterioration, destruction, and recovery of surface films is far more than the thermal intensity. As a result, this type of noise is more easily detectable and is the focus of our investigation. If corrosion is considered a stochastic phenomenon, the corrosion current (potential) at a specific potential (current) can be described as an electrochemical noise, similar to the term 'noise' being used to refer to random, incoherent acoustic or electrical disturbances. Therefore, the time and frequency processing techniques that have been specifically developed for random signals can be utilized. Electrochemical noise, a phenomena that involves the examination of electrical signals in relation to corrosion, has gained significant attention in recent years. The classification of electrochemical noise as random may be subject to debate in certain situations, as a deeper understanding of the process and source of the noise could allow for precise mathematical explanations of the event, rendering it deterministic. The importance of the potential/current variations can be elucidated by considering the transition of a corrosion system from a passive state to a state of corrosion. Under passive

conditions, the potential remains largely constant, with any fluctuations occurring at a sluggish, long-term pace. The occurrence of corrosion in a specific area results in significant and rapid fluctuations in potential and current. This is often characterized by an abrupt decrease in potential, followed by a subsequent exponential recovery. If the conditions intensify, these episodes, referred to as 'glitches', occur more frequently. The occurrence frequency of the 'glitches' is correlated with the size of the electrode area and, more specifically, with the statistical likelihood of a localized film breakdown happening. Given that only a small proportion of the localized events will result in the construction of real pits, the likelihood of a pitting attack remains quite low in this scenario. The primary characteristic of potential change is a gradual decline caused by the formation of a passive coating throughout the entire exposed surface. Every possible alteration, whether it occurs rapidly or gradually declines, is overlaid upon this underlying potential for decline. The entire characterization of the potential fluctuation can be achieved by determining if the single event is stochastic or deterministic in nature. 1) Analysis of film degradation (formation of pits) 2) Kinetics of pit growth The processes of pit growth termination and repassivation kinetics have been thoroughly studied and understood. The scenario is depicted in a schematic manner in the Figure below.

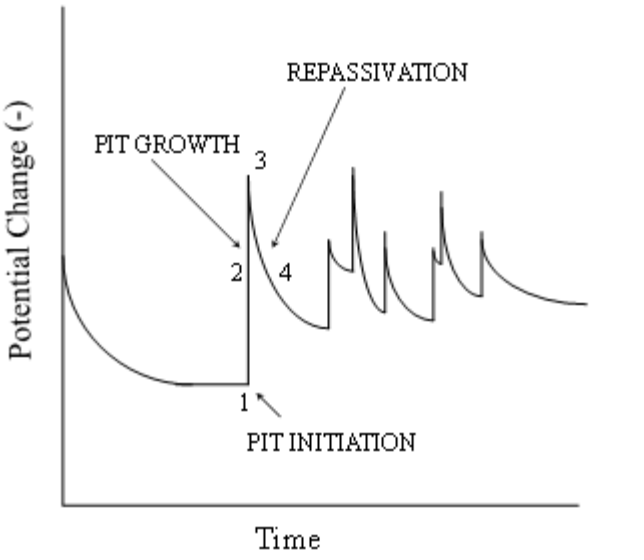

(1)refers the pit initiation (2)refers the pit growth (3) refers the pit growth termination (4) refers the pit repassivation.

Figure 5. Schematic representation of Potential fluctuation during Passive film breakdown and repair

When there are only a few elementary current transients (such as pit nucleation and growth, bubble growth, and departure) that can be observed, a statistical analysis can be performed on the current's time series to determine the average rate at which these transients occur (for example, the pitting rate). However, in scenarios that are more relevant to practical situations, when multiple events occur simultaneously and their current transients overlap, only a spectrum analysis of the random signal may provide an estimation of the distinctive characteristics of the processes. An escalation in the hostility of the surroundings, such as a rise in Cl- concentration, will lead to a higher occurrence rate of events and the fluctuations will seemingly become unpredictable. An analysis based on frequency spectra should demonstrate that the resulting output is a consequence of the overlapping of numerous occurrences. In this scenario, there is a strong likelihood that one or more of these localized breaches in the protective layer may spread and develop into a pit, indicating an eventual occurrence of pitting corrosion.

When there is a complete absence of passivity, meaning that no film is formed, the electrochemical noise output is identical to that of a passive system. This means that there are no recognizable glitches in the output, and any random noise that is there has a low amplitude.

3. Experimental Details

3.1 Electrochemical Potential, Current Noise Measurement

The theory of digital data capture is presented earlier, and this section provides a summary of the practical methods that can be used to execute the theory. These strategies for data collecting and analysis were based on digital procedures that were controlled by a personal computer. These techniques were utilized during the practical work that was included in this thesis. Those programs that the author has written for the purpose of data collecting.

3.1.1 Data Collection Procedures

A history or realization of any process that is recorded over a considerable amount of time is referred to as a time record. A suitable reference electrode and chart recorder can be utilized to quickly accomplish the task of recording the fluctuations in the corrosion potential of an electrode that is corroding freely. Because they represent the process that was recorded at each and every instant of time during the measurement time, time histories that are documented in this manner are considered to be continuous records. It is convenient for the data to be in digital form since data analysis is relatively complicated, and it is also handy for the transformation of the data into the frequency domain. The requirement to digitize a continuous time record, such as a chart recorder time trace, may be avoided if data were captured in digital form, which would be more convenient. As was previously mentioned, there are additional challenges associated with the utilization of the chart recorder. It is necessary to transport information between a recording device, such as a voltmeter, and a processor in order to capture digital data. After that, the data must be stored in order to examine it. A process may only be sampled at intervals, and this sampling must be interpolated in order to realize an accurate representation of the particular process. This is because the amount of time necessary for data transport is finite. An example of a discrete record is a time record that is gathered in this manner. A continuous process is depicted in the accompanying figure, which illustrates the sampling process in this manner.

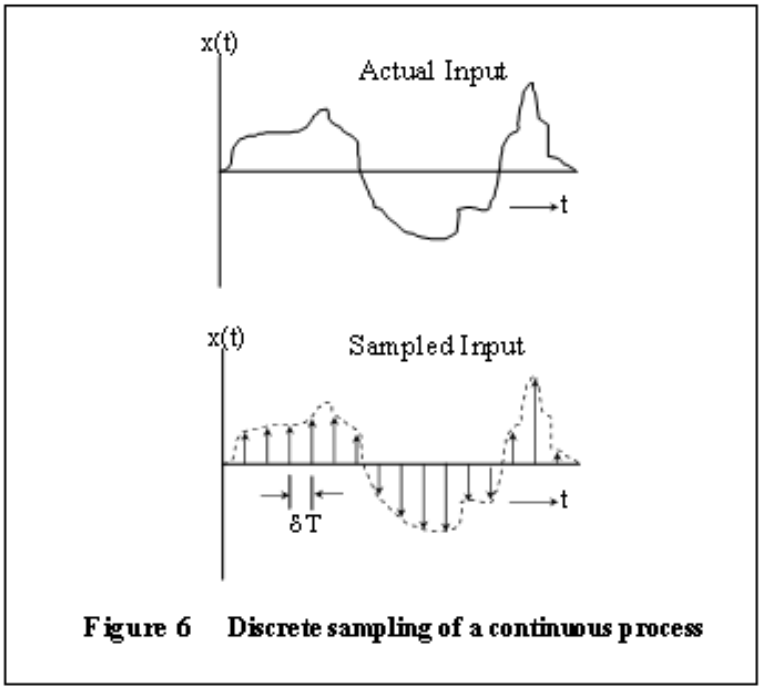

Figure 6 Discrete sampling of a continuous process

When the sample points are placed in close proximity to one another, a sampled representation of a process can be as close to the process as possible. This is accomplished by sampling at a quicker rate, however it is important to note that this will clearly be constrained by the speed of data transfer of the hardware that is involved. It is necessary that the number of points sampled, denoted by the letter N, be sufficient in order to achieve the desired resolution in the frequency domain following the transformation. Frequently utilized for FFT-based data analysis is the Cooley-Tukey Fast Fourier Transform (FFT) algorithm, which necessitates that the data points be a power of two and that N = 1024 (210) be used.

3.1.2 Sampling Rate

Sampling for digital data analysis is typically done at evenly spaced intervals, and it is important to determine a suitable sampling interval, Δt, for collecting any time record. Sampling at points that are too close together, resulting in a fast rate, can lead to data that is highly correlated and redundant. Sampling at a rate that is too high can lead to inaccurate data at lower frequencies when dealing with a time record that has a fixed number of points.If the sampling points are too far apart, meaning the rate is too low, it can lead to the frequency components of interest not being properly resolved in the frequency domain. This phenomenon is known as aliasing and can introduce errors in digital processing. The maximum frequency that can be resolved in the frequency domain with a given sampling interval is determined by the formula: $f_{max} = 1/2\Delta t$. This frequency is commonly referred to as the Nyquist, cut-off, or folding frequency. For a sampling rate of one second (1 Hz), the maximum frequency that can be distinguished in the frequency domain is 0.5 Hz. When the sampling rate is lower than the highest frequency component of a process, that component won't show up in the right place in the frequency domain. Instead, it will be aliased to a lower frequency. Filtering the input signal at a frequency below the sampling frequency can help minimize the error caused by aliasing. The minimum frequency resolution of the spectrum of a discrete time record with N samples can be calculated using the formula: $f_{min} = 1/N\Delta t$. As an analogy, let's consider a materials engineer. Imagine they have 1024 data points that were sampled at one second intervals. This sampling rate gives them a low frequency resolution of 1/1024, which is approximately 0.001 Hz. When studying electrochemical phenomena like pitting, it is generally sufficient to sample a time period of 1024 points at one-second intervals.

3.1.3 Time Record Collection

Electrochemical noise refers to the natural variations in potential or current that occur at an electrode interface. Unlike other techniques that involve applying an external signal to the corroding system, non-perturbed electrochemical methods involve monitoring the corrosion potential and using Zero Resistance Ammeter (ZRA) to measure the galvanic current between two electrodes. The time records collected in this thesis measure the variations in corrosion potential between a working electrode and a reference electrode and the galvanic coupling current flowing between two working electrodes. By utilizing ZRA, we were able to convert the coupling current between the working electrodes into a proportional potential, resulting in the measurement of two potentials with great effectiveness. Once the controlling software has configured the voltmeter, it proceeds to gather data points for a predetermined duration. The program listing can be found in the Appendix.

3.1.4 Noise Measurement at Free Corrosion Potential

Two samples of the same type were used as working electrodes. The two samples were positioned vertically and parallel to each other in the test cell. A reference electrode was positioned between the working electrodes. The potential difference between the sample and reference electrode was measured while the conditions were freely corroding. For measuring the coupling current between two identical samples, a ZRA was connected across the terminals of the samples. The output voltage of the ZRA, which is directly proportional to the input current, was then measured. The connection schematic for both potential and current noise measurements can be found in Figure 7, which will be shown later. For both potential and current noise measurements, a sampling rate of 1 point per second was utilized, and a total of 2048 data points were read. It is important for the number of data points to be a power of 2 (in this case, 2 to the power of 10) to facilitate Fast Fourier transformation. The collected data

were analyzed using statistical methods in the time domain. The records were then converted into the frequency domain using Fast Fourier Transformation (FFT) and Maximum Entropy Method.

For spectral analysis where potential and current fluctuations are correlated in the frequency domain, simultaneous recording of potential and current noise data is necessary.

3.1.5 Instrument Noise Measurement

Despite efforts to eliminate unwanted noise in a system, it is impossible to reduce the inherent noise caused by the fundamental nature of matter. Man-made noise has a unique characteristic of showing periodicity, making it theoretically possible to remove. On the other hand, the second group of noise sources are inherent to the particle-like properties of matter and consistently produce a predictable output in a specific device and operating conditions. The primary sources of these noises are thermal noise, shot noise, and flicker noise, which are covered in the Discussions chapter. Given the unpredictable nature of these events, our ability to make definitive statements is limited to estimating the likelihood and potential impact. Since the instrument noise is influenced by the source impedance of the system being measured, we conducted measurements of the instrument noise with a source resistance of 100 kΩ connected to the inputs of ZRA. Measurements were taken to assess the potential fluctuations between a working electrode and a reference electrode in the solutions used during our tests, as well as in distilled water for comparison purposes. The aim was to determine the level of noise introduced by the reference electrode and the measurement channel.

3.2 Electrochemical Cell

The electrochemical cell employed in this work was a 500 ml beaker open to air with the three electrode system described in the following paragraphs.

3.2.1 Working Electrode

The working electrodes consisted of steel rod samples measuring 4 mm in diameter and 100 mm in length. For optimal results, the specimens underwent mechanical polishing on silicon carbide paper while being rinsed with flowing water. This ensured that any debris on the surface was effectively removed, preventing the formation of surface inclusions and minimizing any potential increase in temperature. The specimens were carefully polished using various grades of silicon carbide paper, washed meticulously with both running water and distilled water, degreased using acetone, and then air dried using an airblower.

3.2.2 Reference Electrode:

Unless otherwise mentioned, all potentials reported were measured with respect to a commercial saturated calomel electrode (SCE).

Uncompensated IR drop

When measuring the potential between the working electrode and reference electrode while current is passing through, there will always be a voltage drop equal to IRs, where Rs represents the solution resistance between the two electrodes, included in the measured potential. The impact of the uncompensated IRs drop on the experiments can vary, ranging from significant to negligible, depending on the experimental conditions and the experiment's requirements. However, it is important to consider at least three possibilities for the effect of IR drop on the results of the experiment in most cases. Firstly, the measured electrode potentials always include an IR drop, resulting in a deviation from the true electrode potential and a potential control error. When the current and solution resistance remain constant, it results in a consistent error that can be subtracted mathematically, as long as the solution resistance is known. Furthermore, when employing linear sweep techniques, the current exhibits a non-linear variation, which can pose challenges in interpreting the obtained results. Additionally, in pulse techniques, the presence of a notable voltage drop causes the increase in potential at the working electrode interface to follow an exponential pattern, which is determined by the time constant of the solution resistance and interface capacitance. IR drop in experiments can be minimised by three main approaches [(3)].

1. Cell Design:

a. Using a Luggin capillary and positioning the Luggin probe in close vicinity to the working electrode.

b. Using a smaller working electrode.

c. Using concentrated supporting electrolyte

2. Simple Arithmetic Correction

If the solution resistance is time-invariant and known by other methods, the real electrode potential for each current can be obtained by subtracting IR_s from the applied potential. This is often used in polarisation experiments.

3. Instrumental Correction:

In the realm of instrumental approaches of IR compensation, the positive feedback method is among the most often used methodologies. The concept behind this method is that a correction voltage that is proportionate to the IRs drop is introduced into the input of the potentiostat. This is done in order to compensate for the inaccuracy in the total applied electrode potential. Furthermore, the electrode potential that was measured is precisely equal to Etrue. When put into practice, however, this approach presents challenges due to the fact that the components of the cell and the amplifiers in the control circuit induce phase shifts. Therefore, there are large time lags between the application of the correction signal, the construction of the correction, and the sensing that the correction has been applied. Depending on the length of these delays, the entire feedback system can end up overcorrecting for changes in the input signal.

3.3 Solutions

For the investigation of the impact of chlorides in pour water, measurements were taken of noise signals in both concrete solution and concrete solution containing 10,000 ppm chloride. The experiments involved the use of a 10,000 ppm chloride solution. Measurements were also taken of the signals in distilled water for comparison.

3.4 Equipment

For accurate measurement of potential and current noise signals, it is essential to use instruments that offer high accuracy and excellent resolution. They need to be able to detect small variations in noise levels, as well as quickly react to sudden changes in transients. By utilizing a compatible interface, the measured values can be seamlessly transmitted to a personal computer, allowing for a continuous time record. The transmitted data can be stored on storage media like floppy disk, allowing for future retrieval and analysis. With the expertise of an electrical engineer, it becomes possible to implement a fully automated data collection system, enabling seamless data storage and analysis.

3.4.1 Zero Resistance Ammeter (ZRA)

Electrochemical noise measurements involve the assessment of the coupling current between two electrodes. Using two identical electrodes is typically beneficial, as stated by R.A Cottis, S.Turgoose, and J.Mendoza-Flores in 1994. In the case of short circuit conditions, the coupling current cannot be accurately measured by a basic ammeter. This is due to the presence of an IRm drop across the ammeter, where Rm represents the meter resistance. By connecting the electrodes through the ZRA, their potentials are brought together, resulting in the observation of current flow that reflects the differences in rates and any fluctuations. This polarization of electrodes will thus cause one electrode to become more anodic and the other more cathodic. R.A Cottis and S.Turgoose,1994. One drawback of this technique is that the current of the ZRA is influenced by factors beyond just the driving force. These factors include the resistance of the circuit, such as the impedance of the electrodes and the resistivity of the electrolyte. Nevertheless, when the electrodes are in close proximity, the outcomes are indistinguishable from the interactions between different sections of a single electrode.

3.4.2 ZRA of ACM Instruments

This high-performance laboratory instrument, the ACM (Applied Corrosion Monitoring Ltd) Instruments ZRA, is specifically designed to accurately measure the galvanic current between two electrodes. These electrodes

simulate a connection with zero resistance wire, allowing for precise monitoring of the potential of the galvanic couple. The device offers buffered current and potential outputs, which were transmitted to the computer via an analog-digital converter. Here is a detailed figure illustrating the experimental setup. Typically, the standards ensure that the measurement method aligns with the research work's benchmark, following ASTM C876-15, 2015 and ASTM G199-09(2020)e1, 2020.

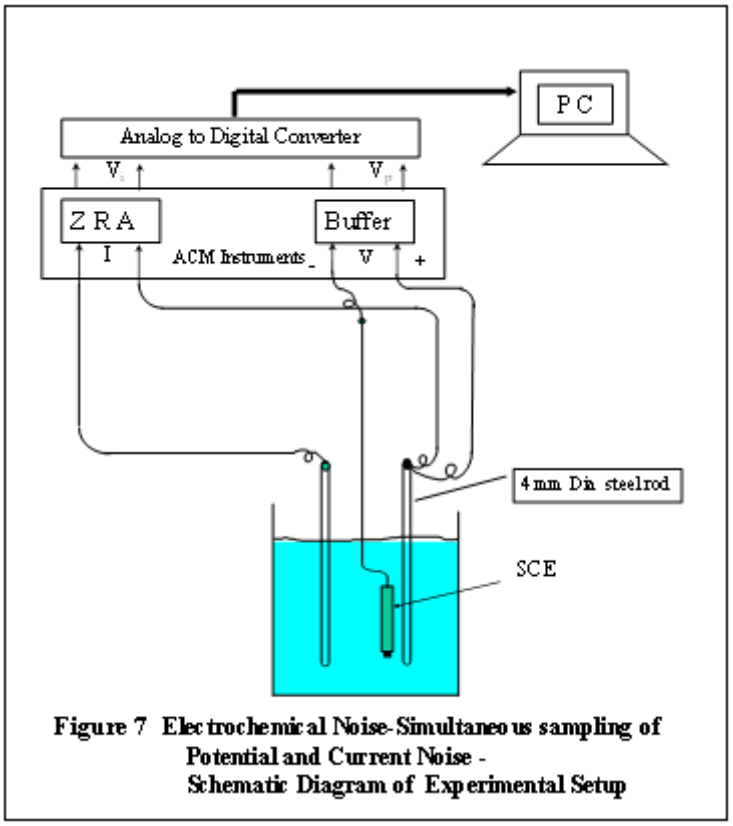

Figure 7 Electrochemical Noise-Simultaneous sampling of Potential and Current Noise - Schematic Diagram of Experimental Setup

4. ANALYSIS METHODS

Signal analysis techniques commonly employed in communication engineering and related fields can also be applied to corrosion systems. Analysis can be conducted either in the time domain or the frequency domain. Here is a brief overview of the analysis techniques. To gain a deeper understanding of digital signal processing and interpretation, it would be beneficial to consult a textbook on the subject. Transforming electrochemical noise data into the frequency domain is a commonly used method for analysis. This approach allows for better separation of desired and undesired components by applying signal processing techniques. One way to extract the desired portion of the signal is by analyzing the instrument's noise spectra without the system being studied, and then subtracting this data from the actual measurements. Nevertheless, if the total signal is only marginally larger than the noise to be subtracted, the fact that the obtained value of instrumental noise is an expected value rather than the actual noise generated could pose a significant limitation. By conducting simultaneous measurements and analyzing the cross power spectrum, more accurate and insightful results can be achieved. The relationship between time and frequency domain analyses can be understood by examining the Fourier transforms. Just like a materials engineer, the conventional spectrum analyzer, whether it's a high-tech instrument or a software package, provides a detailed analysis of complex waveforms by breaking them down into easily observable frequency components. As per a study conducted by Obot, I.B.; Onyeachu, I.B.; Zeino, A.; Umoren, S.A in 2019, it is highlighted that the decomposition plays a crucial role in determining the system's response to a signal. By applying the superposition principle, one can analyze these individual components to understand the overall

behavior. These basic component signals exhibit periodicity and complexity, allowing for the examination of both the system's amplitude and phase. When dealing with a variable like electrochemical noise data that changes over time, Fourier analysis can break it down into different oscillatory functions, each with its own unique frequency. These frequencies, along with their amplitudes and phase angles, make up the frequency components of the original noise signal. From this, we can estimate the pit initiation frequency and corrosion behavior. The Power Spectral Density (PSD), which is obtained by squaring the Fourier Transform, is widely used for analysis purposes. There are different methods available to estimate the PSD, such as Fast Fourier Transforms or the Maximum Entropy Method. While the discrete Fourier transform calculates the coefficients of sinewaves that combine to form the observed time record, the maximum entropy method calculates the coefficients of a specific type of digital filter that would produce the observed time record when used with a white noise input signal. Although the MEM technique naturally yields smooth spectra, the FFT is known to produce spectra with a significant amount of scatter. Therefore, it may be necessary to apply some sort of smoothing.

5. ANALYSIS & DISCUSSION

5.1 Time Domain

Average noise behaviour is typically described by the average noise power, also described as the variance of the potential or current. It is also common to measure the square root of the noise power, $\sqrt{E_n^{\,2}}$, also known as the standard deviation of the potential noise. In order to convert the signal that is subject to drift into a better approximation of a stationary process, a straight line was fitted to the original data, and then the deviation of individual points from the straight line was used as the new 'detrended' data set.

5.2 Frequency Domain

Examining data in the frequency domain reveals characteristics that may not be easily observable in the time domain. Given the presence of both individual charge transfer events and background noise in the instrumentation, it is crucial to conduct the analysis in the frequency domain. For plotting the PSD, we have utilized the unit V2/Hz. This unit is significant as it pertains to the power distribution of the sequence, and the measure of 'amplitude-squared' has the dimensions of power. The terminology used for current noise is essentially the same as that for potential noise. The reported spectral density is given in units of A2/Hz. There are various methods to estimate power spectra, with the Fast Fourier Transform (FFT) and the Maximum Entropy Method (MEM) being the most commonly used techniques for electrochemical noise analysis. With the MEM, you can achieve a smooth spectrum, unlike the FFT which tends to have a significant scatter. However, the FFT has a closer connection to the time record, as it allows for the reconstruction of the time record through inverse transformation. In practice, it has been observed that both methods yield identical information, which is consistent with our own findings. Thus, we utilized MEM to analyze and contrast the various noise signatures.

6. EXPERIMENTAL RESULTS

The time records that have been de-trended, along with their PSD plots that have been calculated using FFT and MEM methods, are utilized. The average potential noise power (variance) of the time record that has been collected, as well as the average potential noise power spectral density at low frequencies up to 0.1 Hz, which has been calculated based on the results of the MEM, are displayed below.

	Potential Noise Power		**Current Noise Power**	
	Time domain	Freq domain (upto 0.1 Hz)	Time domain	Freq domain (upto 0.1 Hz)
	V^2/Hz	**V^2/Hz**	**A^2/Hz**	**A^2/Hz**
Instrument Noise (100 k resistor)	5.966E-10	1.229E-09	1.244E-19	3.168E-19
Distilled Water	8.821E-06	3.382E-05	1.080E-13	5.466E-13
Cement solution-1	9.667E-06	2.654E-05	3.570E-14	1.102E-13

Cement solution 2	2.706E-06	2.167E-05	3.475E-15	1.562E-14
Cement solution + NaCl 10,000 ppm	7.948E-06	8.667E-05	1.129E-13	6.524E-13
Sodium Chloride 10,000 ppm	5.354E-06	3.011E-05	3.507E-12	3.187E-11

7. DISCUSSION

The instrument noise is the minimum noise that is intrinsic to the system due to internal noise sources. Based on a shot noise model [(2)] the average current noise power is related to i_{corr} and q by:

$$\overline{I_n^2} = 2\, q_a\, i_{corr} b$$

By assuming the potential noise to be the result of the current noise acting on the polarisation resistance, R_p, at the low frequency limit and substituting B/i_{corr} for R_p we get the following equations for potential noise:

$$\overline{E_n^2} = R_p^2\, \overline{I_n^2}$$

$$\overline{E_n^2} = 2\, B^2 q_a b / i_{corr}$$

From the above equations, it is seen that the current noise power is directly proportional to i_{corr} whereas the potential noise power is inversely proportional to i_{corr}.

7.1 Potential Noise

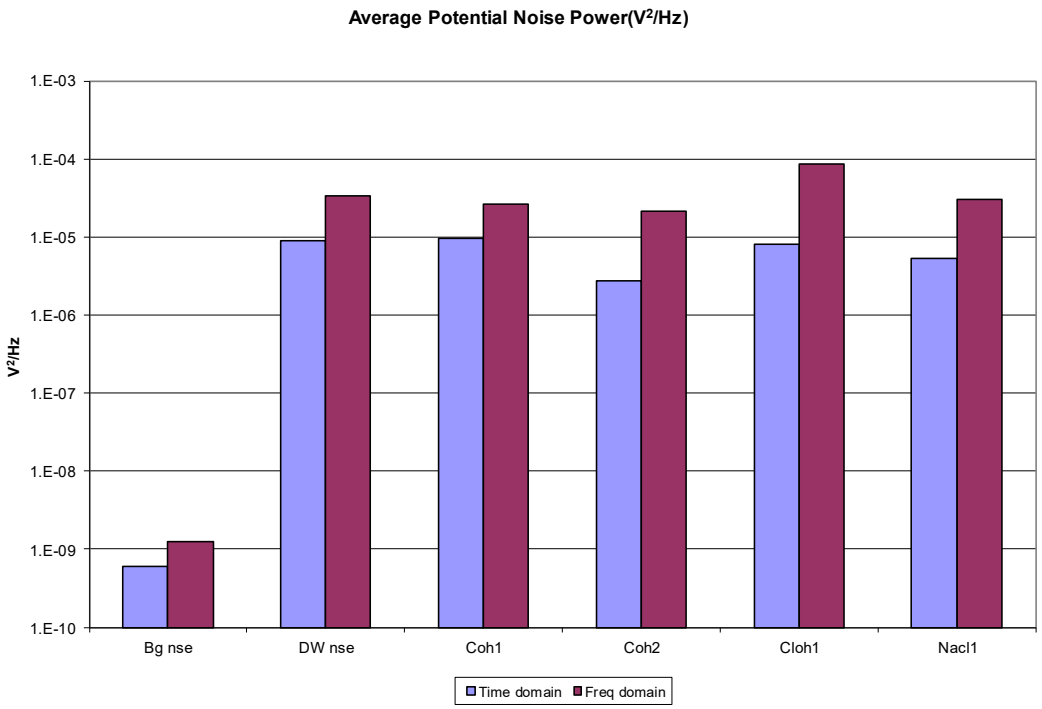

Compared to the actual potential noise, the noise from the instrument is many orders of magnitude lower. After that point, it becomes more challenging to correctly interpret the results and to build a connection between them. The results, on the other hand, make it abundantly evident that the monitoring of potential noise by itself is not sufficient for making any significant predictions regarding the behavior of the localized corrosion. As pits initiate

the increase in the instantaneous pulses of charge causes the potential noise to increase proportionally. However, when pits grow, R_p falls (increase in i_{corr}) and therefore the potential noise either decreases or remains the same depending upon the relative magnitudes of the individual effects. Hence, electrochemical potential noise, by itself, cannot be correlated unambiguously with corrosion rate or even the occurrence of localised corrosion.

7.2 Current Noise

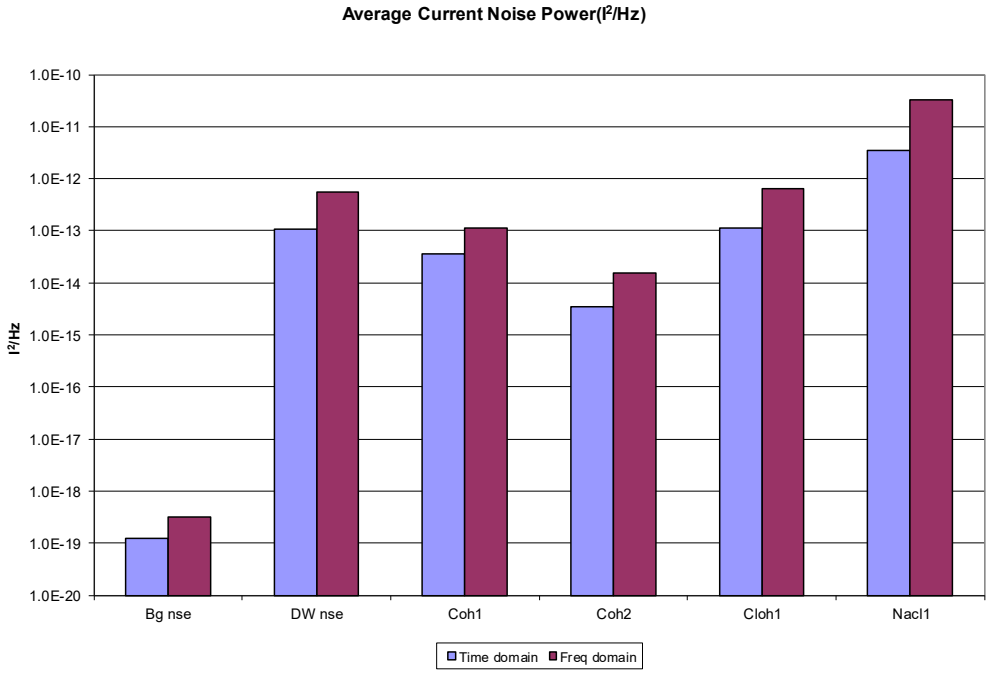

The current noise powers are many orders higher than the background noise. As expected from the shot noise model, the current noise power is higher in solutions containing chloride. The current noise power in cement solution is lower in the cement solution compared to that in distilled water which probably is due to the effect of the passivating iron oxide film which rapidly forms on the steel surface in the presence of moisture, oxygen, and the water soluble alkaline products during the hydration of cement. It appears that the current noise power as well as i_{corr} will decrease progressively as the surface gets coated.

7.3 Estimation of Charge

The dissolution process in an electrochemical reaction can be considered as a series of brief events occurring randomly. For uniform dissolution processes it is expected that the value of charge, q, will correspond to the charge liberated by 10^2 to 10^6 atoms. However, the initiation process of pitting is often found to involve a charge of the order of 10^{-6} C corresponding to about 10^{12} atoms. Therefore, it is expected that the estimation of the charge in the transient will provide a valid parameter for the practical identification of localised corrosion. Conventionally, the calculation of charge exchanged is straightforward and obtained by integrating the current passed over a period of time. If analog chart recorders are used for the noise trace, curve fitting procedures may be used to approximate the growth and decay curves. On the other hand digitised time records do not provide information in the interval between the sampling periods. However, with suitable software one could approximate the growth and decay curves using sophisticated curve fitting techniques. We have not studied the shape of the transients considering the complexity of curve fitting techniques. Moreover, it is difficult to estimate the area under a transient accurately for a sampled time record. Instead, we have attempted to estimate the quantity of the charge in the transient from the statistical properties of the time record. Moreover, an automated analysis capable of coping with many transients is possible using the statistical approach. By considering the parameters at low

frequencies only, the effect of the capacitance is minimised and the impedance of the metal-solution interface is just the polarisation resistance at the low frequency limit. If we consider the potential noise to be the effect of current noise acting on the polarisation resistance (at the low frequency limit) then the statistical parameters from potential noise may also be used in the estimation of charge. Armed with the above assumptions, the electrochemical noise may be described using a shot noise model. The charge, q, can be estimated for the assumed shot noise model at the low frequency limit from the relation [1,2]:

$$q = \frac{\sqrt{\overline{E_n^2}\ x\ \overline{I_n^2}}}{2\,B\,b}$$

The Stern-Geary proportionality constant calculated from the Tafel constants is given as:

$B = \beta_a\beta_c/2.303(\beta_a + \beta_c)$

We have selected Tafel constants, $\beta_a = \beta_c = 118$ mV, giving a Stern-Geary coefficient, B, of about 26 mV. The bandwidth, b, is 0.5 Hz in our case. The following Table shows the calculated values of q for the various test conditions.

	Estimated Charge	
	Time domain	**Freq domain**
	Coulombs	Coulombs
Instrument Noise (100 k resistor)	1.657E-16	3.794E-16
Distilled Water	1.877E-11	8.269E-11
Cement solution-1	1.130E-11	3.290E-11
Cement solution-2	1.865E-12	1.119E-11
Cement solution + NaCl 10,000 ppm	1.821E-11	1.446E-10
Sodium Chloride 10,000 ppm	8.333E-11	5.957E-10

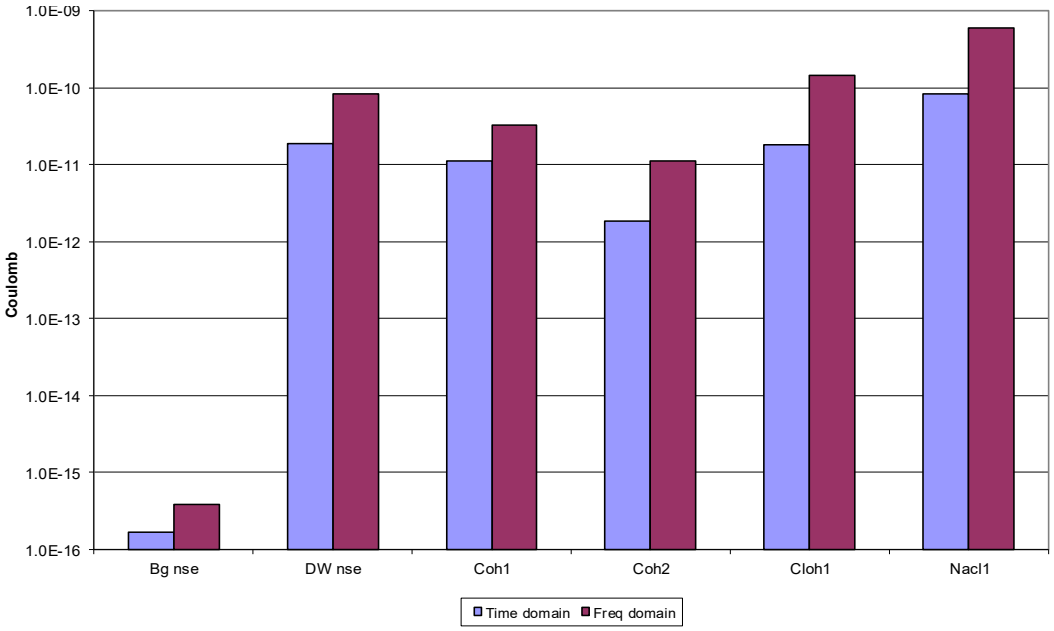

For frequencies that are low enough, individual transients can be considered to be instantaneous pulses, the calculation of charge is based on a shot noise model that is valid for lower frequencies. The calculations that we have done so far for the average potential and current noise power are, however, based on time domain data. This

means that the power from all frequencies, not just the low frequencies, is included in the calculations. We are able to calculate the charge according to the average noise power that is only present in low frequencies thanks to the frequency domain analysis. According to Cottis and others (1), a significant value of q is suggestive of localized corrosion. This idea is based on the shot noise model of electrochemical noise, which was recently proposed. The model appears to be consistent with the results that were presented earlier. In contrast to the other scenarios, the projected charges in the solution that contains chloride are significantly higher. As a result of the creation of a calcium hydroxide passivating coating, the charge in cement solution is lower than the charge in pure water.

7.4 Comparison of q Estimated from the Time & Frequency Domains:

The quantity of charge in the charge transfer event was calculated from the average noise power by the equation:

$$q = \frac{\sqrt{\overline{E_n^2} \times \overline{I_n^2}}}{2\,B\,b}$$

The calculation of q from the time domain make use of the average potential and current noise powers over the entire time period (variance) in the $\sqrt{\overline{E_n^2} \times \overline{I_n^2}}$ part of the equation. Basically the calculation based on the standard deviation is equivalent to the average PSD over the full frequency range of the spectrum. In contrast the frequency domain calculation is based on the low frequency limit, which normally corresponds to the maximum PSD. Hence, we would expect the frequency domain calculation to give the larger value of q, which is confirmed from our results also.

8. CONCLUSIONS

If we consider the fundamental processes underlying the generation of electrochemical noise, a parameter that may be more appropriate is the amount of charge in each transient. Even for uniform dissolution processes occurring as a series of bursts it is expected that the value of q to correspond to the charge liberated by 10^2 to 10^6 atoms. However, the pit initiation process, often found to result in metastable pit nucleation and propagation, gives rise to current transients involving a charge of the order of 10^{-6} C (corresponding to around 10^{12} atoms). Therefore, the electrochemical noise associated with pitting corrosion is much larger than that observed for general corrosion. We have estimated the charge in the transient in the time domain as well as the frequency domain. For the calculations in the frequency domain, the potential and current noise powers contained at low frequencies upto 0.1 Hz only were considered. Various criteria have been developed in the past to assess a material's tendency to localised corrosion based on its electrochemical noise response [(3)]. It remains to be seen which of the above parameters is more appropriate for the practical identification of localised corrosion.

9. FUTURE WORK

The specimen must be inspected using an electron microscope after the test and the topology of the pit studied, and compared with the volume of the pit corresponding to the anodic charge estimated from the potential and current noise powers.

If we make the assumption that the potential noise is a result of the current noise, in which the electrode potential is altered as a result of the action of the current noise on the polarization resistance, then we anticipate that the transients in both the current noise and the potential noise will occur at the same instant, and as a result, we will observe a strong cross-correlation between the two types of noise. Therefore, it would seem logical to employ only the linked potential and current noise powers, rather than the complete spectrum. This would be the case. This kind of correlation analysis will be discussed in our subsequent paper because it is considered to be the second stage, which will then be followed by the third stage, which is the process of converting the phenomena that is being simulated into the practical using the cement and concrete mixture that is currently being used.

REFERENCES

1. Mills, D.J.; Short, N.R. Monitoring Localised Corrosion of Steel in Concrete Using Electrochemical Noise. In Proceedings of the 19th International Corrosion Congress, Granada, Spain, 22–27 September 2002; p. 104. [**Google Scholar**]
2. ASTM C876-15. *Standard Test Method for Corrosion Potentials of Uncoated Reinforcing Steel in Concrete*; ASTM International: West Conshohocken, PA, USA, 2015. [**Google Scholar**] [**CrossRef**]
3. ASTM G199-09(2020)e1. *Standard Guide for Electrochemical Noise Measurement*; ASTM International: West Conshohocken, PA, USA, 2020. [**Google Scholar**] [**CrossRef**]
4. Angst, U.; Elsener, B.; Larsen, C.K.; Vennesland, Ø. Critical Chloride Content in Reinforced Concrete—A Review. *Cem. Concr. Res.* **2009**, *39*, 1122–1138. [**Google Scholar**] [**CrossRef**]
5. Videm, K. Field Studies with Electrochemical Impedance Spectroscopy for Assessing Corrosion of Steel Electrodes in Concrete. In Proceedings of the 19th International Corrosion Congress, Granada, Spain, 22–27 September 2002. Paper no. 730. [**Google Scholar**]
6. Hardon, R.G.; Lambert, P.; Page, C.L. Relationship Between Electrochemical Noise and Corrosion Rate of Steel in Salt Contaminated Concrete. *Br. Corros. J.* **1988**, *23*, 225–228. [**Google Scholar**] [**CrossRef**]
7. Mills, D.J.; Short, N.R. Monitoring Localised Corrosion of Steel in Concrete Using Electrochemical Noise. In Proceedings of the 19th International Corrosion Congress, Granada, Spain, 22–27 September 2002; p. 104. [**Google Scholar**]
8. Mills, D.J.; Mabbutt, S.J.; Short, N.R. A Comparison of Electrochemical Noise and Polarisation Resistance Methods for Monitoring Corrosion of Steel in Concrete. In Proceedings of the EUROCORR 2003, Budapest, Hungary, 28 September–2 October 2003; p. 55. [**Google Scholar**]
9. Legat, A.; Leban, M.; Bajt, Ž. Corrosion Processes of Steel in Concrete Characterized by Means of Electrochemical Noise. *Electrochem. Acta* **2004**, *49*, 2741–2751. [**Google Scholar**] [**CrossRef**]
10. Mariaca, L.; Bautista, A.; Rodriguez, P.; Gonzalez, J.A. Electrochemical Noise for Studying the Rate of Corrosion of Reinforcements Embedded in Concrete. *Mater. Struct.* **1997**, *30*, 613–617. [**Google Scholar**] [**CrossRef**]
11. García-Contreras, J.; Gaona-Tiburcio, C.; López-Cazares, I.; Sanchéz-Díaz, G.; Ibarra Castillo, J.C.; Jáquez-Muñoz, J.; Nieves-Mendoza, D.; Maldonado-Bandala, E.; Olguín-Coca, J.; López-León, L.D.; et al. Effect of Cathodic Protection on Reinforced Concrete with Fly Ash Using Electrochemical Noise. *Materials* **2021**, *14*, 2438. [**Google Scholar**] [**CrossRef**] [**PubMed**]
12. Permeh, S.; Lau, K.; Duncan, M.; Simmons, R. Identification of Steel Corrosion in Alkaline Sulfate Solution by Electrochemical Noise. *Mater. Corros.* **2021**, *72*, 1456–1467. [**Google Scholar**] [**CrossRef**]
13. Xia, D.H.; Song, S.; Behnamian, Y.; Hu, W.; Cheng, Y.F.; Luo, J.L.; Huet, F. Electrochemical Noise Applied in Corrosion Science: Theoretical and Mathematical Models towards Quantitative Analysis. *J. Electrochem. Soc.* **2020**, *167*, 081507. [**Google Scholar**] [**CrossRef**]
14. Lambert, P. *Reinforced Concrete: The History, Properties and Durability of Reinforced Concrete*; Corrosion Prevention Association: Bordon, UK, 2018; Technical Note No.1. [**Google Scholar**]
15. Elsener, B. Half-Cell Potential Measurements—Potential Mapping on Reinforced Concrete Structures. *Mater. Struct.* **2003**, *36*, 461–471. [**Google Scholar**] [**CrossRef**]
16. TR60. *Electrochemical Tests for Reinforcement Corrosion*; The Concrete Society: Camberley, UK, 2004; ISBN 1904482074. [**Google Scholar**]

17. ASTM C876-15. *Standard Test Method for Corrosion Potentials of Uncoated Reinforcing Steel in Concrete*; ASTM International: West Conshohocken, PA, USA, 2015. [**Google Scholar**] [**CrossRef**]

18. ASTM G199-09(2020)e1. *Standard Guide for Electrochemical Noise Measurement*; ASTM International: West Conshohocken, PA, USA, 2020. [**Google Scholar**] [**CrossRef**]

19. Jamali, S.S.; Mills, D.J. A Critical Review on Electrochemical Noise Measurement as a Tool for Evaluation of Organic Coatings. *Prog. Org. Coat.* **2016**, *95*, 26–37. [**Google Scholar**] [**CrossRef**] [**Green Version**]

20. Obot, I.B.; Onyeachu, I.B.; Zeino, A.; Umoren, S.A. Electrochemical Noise (EN) Technique: Review of Recent Practical Applications to Corrosion Electrochemistry Research. *J. Adhes. Sci. Technol.* **2019**, *33*, 1453–1496. [**Google Scholar**] [**CrossRef**]

21. Obot, I.B.; Onyeachu, I.B.; Zeino, A.; Umoren, S.A. Electrochemical Noise (EN) Technique: Review of Recent Practical Applications to Corrosion Electrochemistry Research. *J. Adhes. Sci. Technol.* **2019**, *33*, 1453–1496. [**Google Scholar**] [**CrossRef**]

22. M.G. Pujar, T. Anita, H. Shaikh, R.K. Dayal, H.S. Khatak,Analysis of Electrochemical Noise (EN) Data Using MEM for Pitting Corrosion of 316 SS in Chloride Solution,International Journal of Electrochemical Science,Volume 2, Issue 4,2007,Pages 301-310,ISSN 1452-3981,

23. https://doi.org/10.1016/S1452-3981(23)170751. (https://www.sciencedirect.com/science/article/pii/S1452398123170751)

24. Jiyue Hu, Siyu Wang, Yiyan Lu, Shan Li,Electrochemical noise analysis of cathodically protected steel reinforcement in concrete using carbon fiber sheet as anode,Construction and Building Materials,Volume 313,2021,125474,ISSN 0950-0618.

25. Akib Jabed, Md Mahamud Hasan Tusher† , Md. Shahidul Islam Shuvo, and Alisan Imam, Corrosion of Steel Rebar in Concrete: A Review, CORROSION SCIENCE AND TECHNOLOGY, Vol.22, No.4(2023), pp.273~286